

Sparsity-aware adaptive block-based compressive sensing

ISSN 1751-9675

Received on 29th March 2016

Revised 23rd June 2016

Accepted on 21st July 2016

E-First on 26th August 2016

doi: 10.1049/iet-spr.2016.0176

www.ietdl.org

Seyed Hamid Safavi¹, Farah Torkamani-Azar¹ 

¹Department of Electrical Engineering, Cognitive Communication Research Group, Shahid Beheshti University, Tehran, Iran

✉ E-mail: f-torkamani@sbu.ac.ir

Abstract: Conventional methods for block-based compressive sensing consider an equal number of samples for all blocks. However, the sparsity order of blocks in natural images could be different and, therefore, a various number of samples could be required for their reconstruction. In this study, the authors propose an adaptive block-based compressive sensing scheme, which collects a different number of samples from each block. The authors show that by adapting the sampling rate, in addition to reducing the whole required number of measurements, the reconstruction performance would be improved, simultaneously. Simulation results verify the effectiveness of the proposed scheme, especially for multi-level pixel value images like Mondrian test image.

1 Introduction

The high Nyquist sampling rate in the most of the important and emerging applications of multidimensional signals such as multi-view imaging, hyperspectral imaging and distributed systems, is not desirable. However, many natural signals (e.g. image and video signals) exhibit sparsity features in some properly transformed domain that can be exploited to reduce the required number of samples for reconstruction. Compressive sensing (CS) [1–4] is an emerging technique that benefits from sparsity as a side information. CS directly measures the part of the sparse signals which have information. Hence, the acquisition and compression steps are integrated and signals can be reconstructed with far fewer samples.

Multidimensional signals are usually recast as one-dimensional (1D) vectors and then 1D CS is applied to the result. In spite of sub-Nyquist sampling rate, the required number of measurements for such signals could be still high in CS. There are also some disadvantages in converting a multidimensional signal to very long 1D vectors: (i) inefficient use of the existed structure in all of the signal dimensions because of removing spatial correlation; (ii) huge memory requirement to store the large-size measurement matrices; (iii) complicated construction of sparsifying bases; (iv) computationally expensive reconstruction process.

The idea of block-based CS (BCS) is to overcome some of these challenges [5–7]. Furthermore, the use of Kronecker product matrices in CS is proposed to efficiently model the existed structure in all dimensions of the signal [8, 9]. Moreover, generalised tensor CS (GTCS) is another approach which preserves the intrinsic structure of the tensor data [10]. However, the Kronecker CS and the GTCS approaches are computationally complex compared with multidimensional approaches based on BCS.

To start our definition, three important parameters should be defined: The length of the original signal is assumed to be N , the number of measurement samples of the original signal is denoted by M and the sparsity order of the original signal is considered as k . Measurement matrices satisfy restricted isometry property constraint with high probability if the number of measurements was, at least, equal to $M = \mathcal{O}(k\log(N/k))$, where N is the length of the signal and $k \ll N$ represents the order of the sparsity [3]. Hence, a priori knowledge about the sparsity order of input images is needed to calculate the required number of measurements. Since a priori knowledge is not available, in practice, the upper bound on sparsity order is used. However, the necessary number of samples

might be smaller than the obtained upper bound. In applications like magnetic resonance imaging in which the acquisition process is time consuming and expensive, reducing the required samples for reconstruction, as much as possible is of great importance. With this aim, there is an alternative sequential method for CS which continues to get measurements until reconstruction error becomes smaller than the predefined threshold [11]. However, since this approach solves an optimisation problem when each new measurement is acquired, it has high computational complexity compared with non-sequential approaches. Hence, finding an approach that uses the lower number of measurements with low computational complexity for reconstruction is of great interest.

In the BCS approach, the image is split into the smaller blocks and the required number of samples for reconstruction is assumed to be equal for all blocks. We know that the sparsity order of each block determines the required number of samples for reconstruction. Due to the different sparsity order of blocks in natural images, assuming a distinct number of samples for each block could be more efficient. In this way, the existed structure of sparsity in the image would be better used.

Furthermore, compressible signals such as natural images are not exactly sparse and, in this case, zero norm may not be a desirable measure of sparsity. Hence, a better sparsity measure is needed. This measure should select enough significant coefficients as a sparsity order and can be estimated from a little number of linear measurements. *Numerical sparsity* is one of these efficient sparsity measures which is introduced in [12]. Moreover, in [13], some other sparsity measures like *Gini index* are introduced.

In a nutshell, our contributions in this paper are twofold:

- *New adaptive BCS approach:* In this paper, our aim is to reduce the number of samples as much as possible. Natural images, when partitioned into blocks, have different sparsity pattern in each block. Therefore, we propose to set the size of the sensing matrix for each block based on sparsity order of the block itself and not based on sparsity order of the whole image. With this adaptive selection of a number of samples for each block, we will show that the whole number of samples would be allocated efficiently in blocks. If one block needs more (less) samples, we assign that block more (less) samples and with this simple idea, we will reach to better results.
- *Comparing results of different sparsity measures for our proposed adaptive BCS approach:* Since zero norm is not a good measure of the compressible signals sparsity, it is most important to find efficient sparsity measure for them. In this

paper, we compare the performance of our proposed BCS approach using two popular sparsity measures: i.e. numerical sparsity and Gini index.

Note that compared with BCS, our approach should have an initial step as the estimation of sparsity order for each block. This could add computational complexity to our approach, however, in this paper, the assumption of awareness about the sparsity order (e.g. numerical sparsity, Gini index) of images is used. The estimation error of sparsity measure can adversely affect the performance of our proposed approach. In future, we will try to find a sparsity measure that can be estimated by a low number of measurements. We will also develop an efficient estimation approaches with lower estimation error.

The rest of this paper is organised as follows. Section 2 describes BCS. Section 3 presents motivation of our work and explains our proposed adaptive BCS scheme. In Section 4, we have evaluated the performance of sparsity-aware adaptive BCS approach with some simulations. Finally, Section 5 concludes the paper.

2 Block-based CS

Consider an image $\mathbf{x} \in \mathbb{R}^{N_r \times N_c}$ which is partitioned into $B \times B$ blocks. Let \mathbf{x}_j denote j th block ($j = 1, \dots, L$, where $L = (N/B^2)$) of input image \mathbf{x} through raster scanning. In BCS, all blocks are sampled with same measurement matrix Φ_B . Therefore, the sampled measurements vector can be written as $\mathbf{y}_j = \Phi_B \mathbf{x}_j^{\text{vec}}$, where $\mathbf{x}_j^{\text{vec}}$ is the vectorised version of \mathbf{x}_j and Φ_B denotes the $M_B \times N_B$ orthonormal measurement matrix with $N_B = B^2$ and $M_B = \lfloor (M/N)B^2 \rfloor$, where M is the required number of measurements for reconstruction of the whole image. Also, we assume that $\mathbf{x}_j^{\text{vec}}$ is sparse in some proper transform domain like discrete cosine transform (DCT), i.e. $\mathbf{x}_j^{\text{vec}} = \Psi_B \mathbf{s}_j^{\text{vec}}$, where $\mathbf{s}_j^{\text{vec}}$ is the sparse representation of the $\mathbf{x}_j^{\text{vec}}$ and Ψ_B is sparsifying basis of each block. Hence, the global measurement matrix Φ and consequently the global sparsifying basis Ψ can be written as follows:

$$\Phi = \begin{bmatrix} \Phi_B & \mathbf{0} & \dots & \mathbf{0} \\ \mathbf{0} & \Phi_B & \dots & \mathbf{0} \\ \vdots & \vdots & \ddots & \vdots \\ \mathbf{0} & \mathbf{0} & \dots & \Phi_B \end{bmatrix} \quad (1)$$

$$\Psi = \begin{bmatrix} \Psi_B & \mathbf{0} & \dots & \mathbf{0} \\ \mathbf{0} & \Psi_B & \dots & \mathbf{0} \\ \vdots & \vdots & \ddots & \vdots \\ \mathbf{0} & \mathbf{0} & \dots & \Psi_B \end{bmatrix} \quad (2)$$

Comparing the measurement matrix for each block Φ_B with global measurement matrix Φ shows that the size of the matrix that should be stored is greatly decreased. Besides, the encoder does not need to wait until the entire image is measured. In fact, choosing the proper size of blocks is most important and it determines the computational complexity of reconstruction of each block. However, one unpleasant consequence of using BCS is the appearance of blocking artefact which degrades the performance and should be avoided. Due to the blocking artefact appearance, the size of the blocks could not be assumed to be much smaller.

To speed up the reconstruction process, we use the smoothed projected Landweber (SPL) approach [6]. In addition, Wiener filter is applied to remove blocking artefacts. Similar to [6], we call the whole acquisition and reconstruction process BCS-SPL hereafter.

3 Proposed sparsity-aware adaptive BCS

3.1 Designing structurally sensing matrix

Block diagonal structure of measurement matrix in BCS is more efficient compared with other popular approaches. Hence, this brings to mind the question that are there other structures that can yield better performance than block diagonal structure? In fact, the answer is yes, but, finding the structurally optimal sensing matrix has still not been answered. In this section, our aim is to design structurally efficient sensing matrix. The designed sensing matrix in (1), which originally proposed in [5], has assumed the equal number of samples for each block which is the result of equal sparsity order assumption for each block. However, natural images have different sparsity pattern in each block. Hence, we first manually generate a test image like Fig. 1a which the sparsity order of it is known already. Therefore, we could investigate the performance of our proposed approach on this test image.

Let us explain our proposed approach. We have used the same approach in [6] with a difference in designing sensing matrix for each block. Contradictory to [5, 6] we set the size of sensing matrix for each block (Φ_B) based on the sparsity order of the block itself. Mathematically, we replace the sensing matrix of each block (Φ_B) with Φ_{B_ℓ} for $\ell = 1, \dots, L$ which Φ_{B_ℓ} is an $M_{B_\ell} \times N_B$ orthonormal measurement matrix with $M_{B_\ell} = ck_{B_\ell} \log(N_B/k_{B_\ell})$ for some constant c , where k_{B_ℓ} is the sparsity order of ℓ th block

$$\Phi = \begin{bmatrix} \Phi_{B_1} & \mathbf{0} & \dots & \mathbf{0} \\ \mathbf{0} & \Phi_{B_2} & \dots & \mathbf{0} \\ \vdots & \vdots & \ddots & \vdots \\ \mathbf{0} & \mathbf{0} & \dots & \Phi_{B_L} \end{bmatrix} \quad (3)$$

$$\Psi = \begin{bmatrix} \Psi_{B_1} & \mathbf{0} & \dots & \mathbf{0} \\ \mathbf{0} & \Psi_{B_2} & \dots & \mathbf{0} \\ \vdots & \vdots & \ddots & \vdots \\ \mathbf{0} & \mathbf{0} & \dots & \Psi_{B_L} \end{bmatrix} \quad (4)$$

Fig. 1a shows an image of size 128×128 which is 320 sparse. We have partitioned this image into blocks with size 32×32 . Fig. 1b represents sparsity order of each block and the required number of measurements ($M_B = ck_B \log(N_B/k_B)$ with $c = 2$ [12]) for reconstructing the each block. Figs. 1c and d show the reconstructed image with BCS-SPL approach [6] and the proposed sparsity-aware adaptive BCS-SPL approach which uses the mentioned number of measurements in Fig. 1b, respectively. Conventional block-based approaches assign fixed and an equal number of measurements for all blocks. In this case, it is probable that for each block the assigned number of samples be low or high. Therefore, the sampling rate for each block should be chosen adaptively. Comparing the proposed approach with the conventional BCS-SPL approach, we find that it is possible to achieve better performance with an adaptive selection of sampling rate of each block even using the lower number of measurements. In other words, the number of measurements for each block was assigned more efficiently. Moreover, it could be seen from this figure that the visual quality of the blocks with higher sparsity order in our proposed approach is better than the conventional approach, however, as we assign a lower number of samples for blocks with lower sparsity order, the visual quality of these blocks become lower than conventional approach. In this case, may be it is needed to consider a lower bound for the number of measurements relative to the block size or even the quality of the original block. In the future, we will investigate this case.

3.2 Different measures of sparsity

As we mentioned earlier, compressible signals are approximately sparse and zero norm is not a good measure for sparsity order of them. For real images which are compressible in some transform basis, we should know the sparsity order of each block to choose

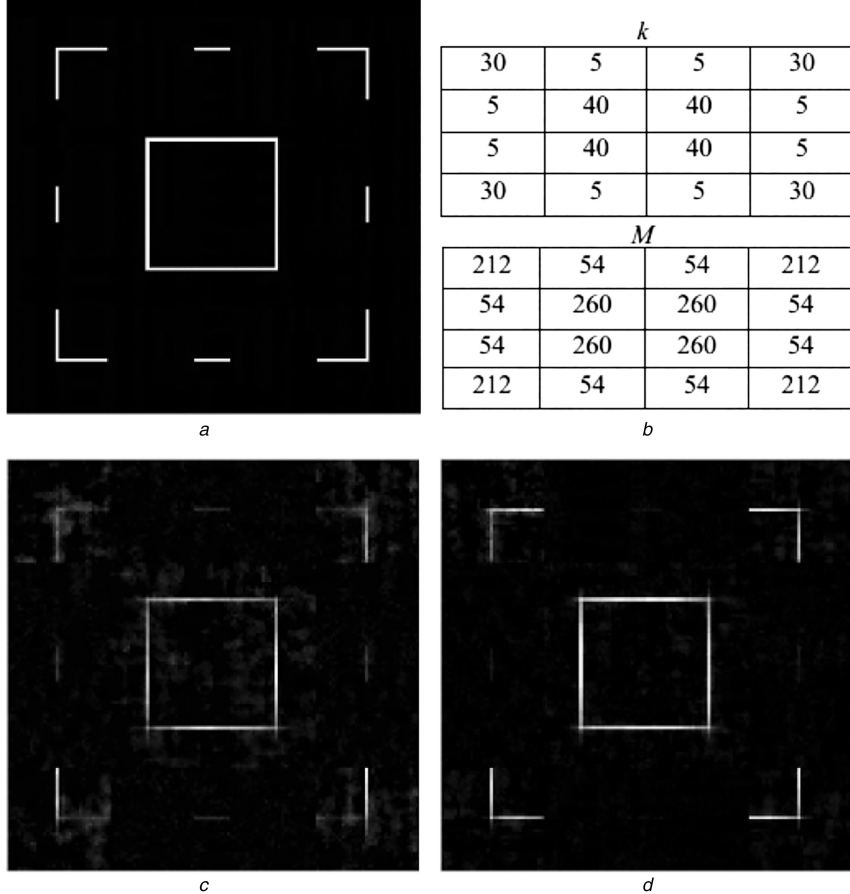


Fig. 1 Original image and reconstructed images

(a) Original image ($K=320$, $N=128 \times 128$), (b) Sparsity order and number of measurement considered for reconstruction in each block, (c) Reconstructed image, BCS-SPL [6] (PSNR = 21.25 dB and $M=2520$), (d) Reconstructed image, sparsity-aware adaptive BCS-SPL (PSNR = 22.9 dB and $M=2320$)

the correct number of measurements for each block. Therefore, we need an efficient sparsity measure which should select enough significant coefficients as a sparsity order. Consider a non-zero signal vector $\mathbf{x} \in \mathbb{R}^N$, where N denotes the signal size. Numerical sparsity is one of the mostly used sparsity order measures that is introduced in [12] as follows:

$$S(\mathbf{x}) = \frac{\|\mathbf{x}\|_1^2}{\|\mathbf{x}\|_2^2} \quad (5)$$

which is the lower bound on zero norm for all non-zero \mathbf{x} . Furthermore, some sparsity measures were introduced in [13]. It is proved that between the different sparsity measures, Gini index is the only measure that has all of the favourable properties defined in [13]. Hence, let us introduce Gini index: given a vector $\mathbf{x} = [x_1 \ x_2 \ \dots \ x_N]$, we order from smallest to largest, $x_{(1)} \leq x_{(2)} \leq \dots \leq x_{(N)}$, where (1), (2), ..., (N) are the new indices after the sorting operation. The Gini index is given by

$$\text{Gini}(\mathbf{x}) = 1 - 2 \sum_{j=1}^N \frac{x_{(j)}}{\|\mathbf{x}\|_1} \left(\frac{N-j+0.5}{N} \right) \quad (6)$$

We should mention that the value of Gini index does not give us exact sparsity order, but it is a normalised index between 0 (least sparse) and 1 (most sparse) that is favourite for our adaptive allocation of samples between blocks.

In summary, the number of samples is assigned to each block based on Table 1 for different sparsity measures. As can be seen from this table, the way that we have assigned the samples to blocks for Gini index is quite different from numerical sparsity. Since Gini index did not give us the exact sparsity order (k), in this case, we have assigned the number of measurements for each block proportional to Gini index of each block itself and not based on the required number of measurements for reconstruction.

4 Simulation results

In this section, we have provided extensive simulations to demonstrate the effectiveness of knowledge about sparsity order of blocks and adaptively allocation of a number of the measurements to blocks based on them. We have used DCT as a sparsifying basis for images. Figs. 2 and 3 compare the average peak signal-to-noise ratio (PSNR) and structural similarity (SSIM) [14] of different test images such as Mondrian (512×512), Tile roof (512×512), Clock (256×256), Lenna (512×512), Barbara (512×512) and Cameraman (256×256) versus required number of measurements for 50 independent trials, respectively. In these figures, the block size is assumed to be 32×32 . We choose Mondrian, Tile roof and Clock test images, because of multi-level pixel value nature of

Table 1 Number of samples allocated for each block

Conventional BCS	Proposed approach with numerical sparsity	Proposed approach with Gini index
$M_B = \frac{1}{L} \times M$	$M_{B_l} = \frac{k_{B_l} \log(N_B/k_{B_l})}{\sum_{j=1}^L k_{B_j} \log(N_B/k_{B_j})} \times M$	$M_{B_l} = \frac{1 - \text{Gini}(x_l)}{\sum_{j=1}^L (1 - \text{Gini}(x_j))} \times M$

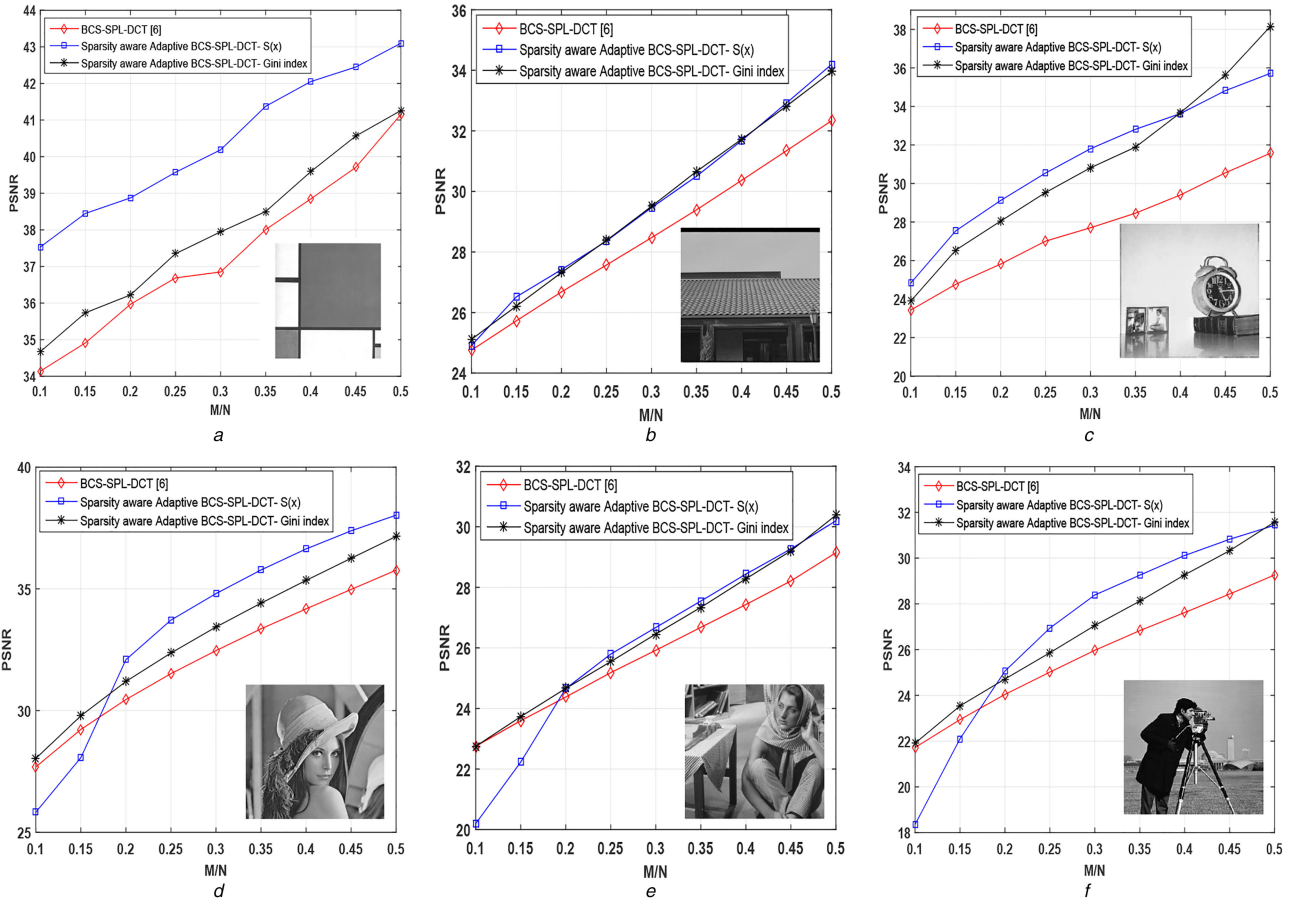


Fig. 2 PSNR versus normalised measurements for different test images

(a) Mondrian, (b) Tile roof, (c) Clock, (d) Lenna, (e) Barbara, (f) Cameraman

these test images, which we expect the better result for this type of images for our proposed approach. As we can see, the performance of the proposed approach is better than the conventional block-based scheme in terms of PSNR and SSIM. Also, compared with [5], we have reached the $\text{PSNR} = 39.5 \text{ dB}$ at $M/N = 0.25$ for Mondrian test image, which is 3 dB higher than the best result of [5] at the same measurement rate. Hence, designing structurally efficient sensing matrix could greatly improve the performance.

To show that why our proposed sparsity-aware adaptive BCS-SPL approach is better for the Mondrian, Tile roof and Clock test images, we compare their self-similarity. If there exists self-similarity in the image, in other words the image has the same texture on the entire image, then our proposed approach can always achieve better performance even using low number of measurements. To investigate this property, we divide the image into blocks (with size $B \times B$) and compute their covariance matrices and then its B eigen-blocks. Now all blocks could project to these eigen-blocks and provide $B \times 1$ vector. If these projected vectors are correlated or similar, then it could be resulted that all blocks have the same texture and then their sparsity levels are close to each other. If these projected vectors are not similar, these blocks have different texture and hence, their sparsity levels are more different. We compute the projected vector's entropy to compare, but this comparison could be done in different forms. Fig. 4 shows the self-similarity for the different test images. As can be seen from this figure, there exists more similar blocks in the Mondrian, Tile roof and Clock test images compared with the Lenna, Barbara and Cameraman test images.

It is also observed that the performance of the proposed approach using Gini index as a sparsity measure is always better than the conventional BCS. Our proposed approach using numerical sparsity is the best approach for multi-level pixel value images like Mondrian, Clock and Tile roof test images; meanwhile, this is true for Lenna, Barbara and Cameraman test images just in case that the sampling ratio is higher than 0.2. This is because of the logarithmic nature of the required number of samples. We have

also compared the required number of samples for each block for different approaches in Fig. 5. Consider the first row of this figure, i.e. the Mondrian, Tile roof and Clock test images which have more similar blocks. As can be seen from this figure, the required number of measurements for each block for our proposed approach using numerical sparsity and Gini index are not changed a lot from one block to another one (because more similar blocks exist in these images). Now, consider the second row of Fig. 5, i.e. the Lenna, Barbara and Cameraman test images which have less similar blocks. In this case, the required number of measurements for each block using our proposed approach with numerical sparsity is changed a lot. It is necessary to mention that, since Gini index is a normalised sparsity measure index and does not have a logarithmic nature in allocation of measurements, hence, the required number of measurements for each block is not changed a lot for this case. As a result, for the images that have less similar blocks, when the number of available measurements is small, we could not provide exact required number of measurements for some blocks in our proposed approach using numerical sparsity.

Finally, in order to show the impact of block size (B) on the performance of our proposed approach, the PSNR versus block size for fixed number of measurements is plotted in Fig. 6. As mentioned before, one unpleasant consequence of using BCS is the appearance of blocking artefact which degrades the performance and should be avoided. Therefore, using small-size blocks, the number of blocks in the original image increase and this intensifies the blocking artefacts. Hence, as expected, it is observed that the performance is better for large-size blocks compared with smaller one.

5 Conclusions and future work

In this paper, we proposed an adaptive BCS scheme. First, we showed that the sparsity order of each block in an image could be different. As a result, the required number of measurements for each block would be different. Hence, we have selected a distinct

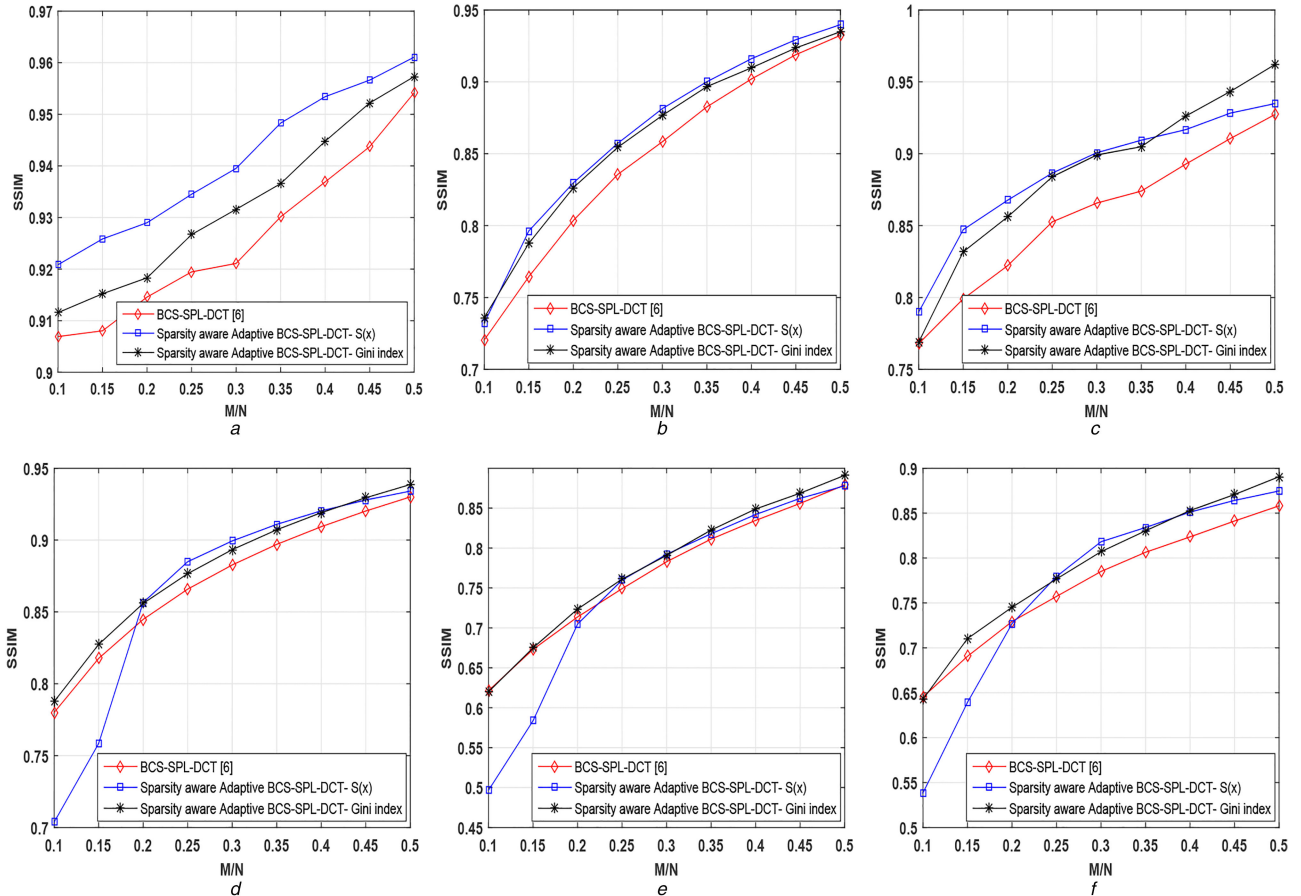


Fig. 3 SSIM versus normalised measurements for different test images

(a) Mondrian, (b) Tile roof, (c) Clock, (d) Lenna, (e) Barbara, (f) Cameraman

sampling rate for each block. Then, we compared the performance of our proposed approach for two popular sparsity measures, i.e. numerical sparsity and Gini index and the superiority of numerical sparsity was shown. Simulation results verified the efficiency of the proposed scheme. Finally, there are several lines of research arising from this work which include finding sparsity measures that could be estimated from low number of measurements and work well with all input images. Moreover, the question of finding the structurally *optimal* sensing matrix has still not been answered.

6 Acknowledgment

The authors thank the anonymous reviewers and the editor for their insightful comments and suggestions to improve the quality of the paper.

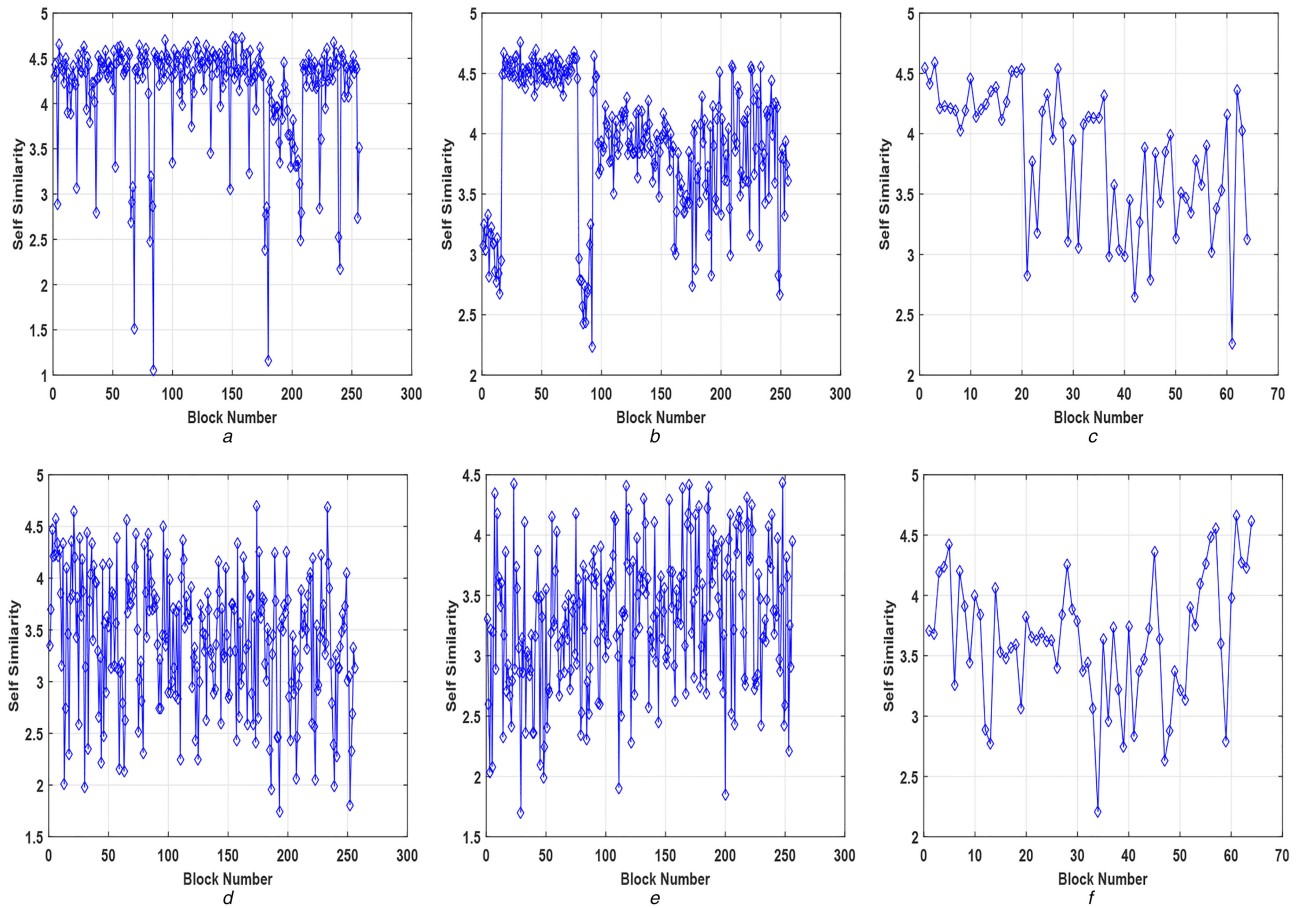


Fig. 4 Self-similarity for different test images

(a) Mondrian, (b) Tile roof, (c) Clock, (d) Lenna, (e) Barbara, (f) Cameraman

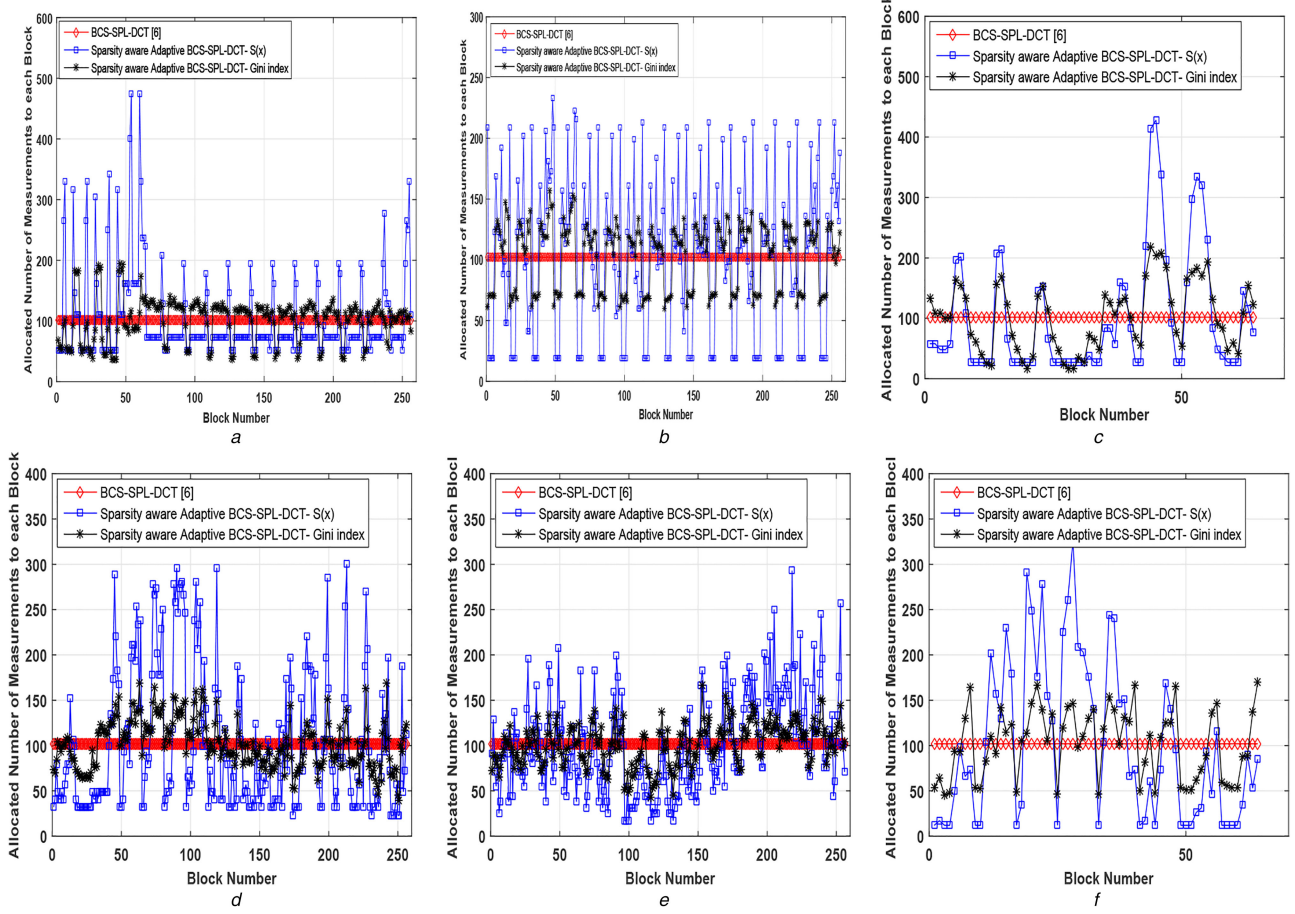


Fig. 5 Required number of measurements for each block when $M/N = 0.1$ for different test images

(a) Mondrian, (b) Tile roof, (c) Clock, (d) Lenna, (e) Barbara, (f) Cameraman

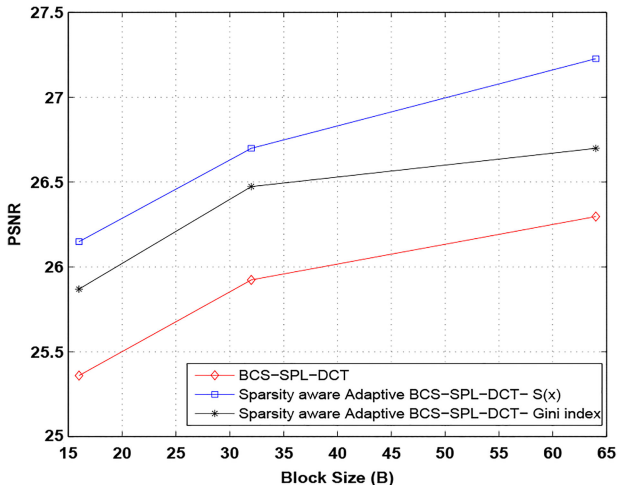


Fig. 6 PSNR versus block size for Barbara test image ($M/N = 0.3$)

7 References

- [1] Donoho, D.L.: ‘Compressed sensing’, *IEEE Trans. Inf. Theory*, 2006, **52**, (4), pp. 1289–1306
- [2] Candes, E.: ‘Compressive sampling’. Proc. of the Int. Congress of Mathematicians, Madrid, Spain, 2006, pp. 1433–1452
- [3] Baraniuk, R.G.: ‘Compressive sensing [lecture notes]’, *IEEE Signal Process. Mag.*, 2007, **24**, (4), pp. 118–121
- [4] Davenport, M.A., Duarte, M.F., Eldar, Y.C., et al.: ‘Introduction to compressed sensing’, 2011, vol. **93**, 1, pp. 1–64
- [5] Gan, L.: ‘Block compressed sensing of natural images’. 15th IEEE Int. Conf. on Digital Signal Processing, 2007, pp. 403–406
- [6] Mun, S., Fowler, J.E.: ‘Block compressed sensing of images using directional transforms’. 16th IEEE Int. Conf. on Image Processing (ICIP), 2009, pp. 3021–3024
- [7] Fowler, J.E., Mun, S., Tramel, E.W.: ‘Block-based compressed sensing of images and video’, *Found. Trends Signal Process.*, 2012, **4**, (4), pp. 297–416
- [8] Duarte, M.F., Baraniuk, R.G.: ‘Kronecker compressive sensing’, *IEEE Trans. Image Process.*, 2012, **21**, (2), pp. 494–504
- [9] Ghaffari, A., Babae-Zadeh, M., Jutten, C.: ‘Sparse decomposition of two dimensional signals’. IEEE Int. Conf. on Acoustics, Speech and Signal Processing (ICASSP), 2009, pp. 3157–3160
- [10] Friedland, S., Li, Q., Schonfeld, D.: ‘Compressive sensing of sparse tensors’, *IEEE Trans. Image Process.*, 2014, **23**, (10), pp. 4438–4447
- [11] Malioutov, D.M., Sanghavi, S.R., Willsky, A.S.: ‘Sequential compressed sensing’, *IEEE J. Sel. Top. Signal Process.*, 2010, **4**, (2), pp. 435–444
- [12] Lopes, M.: ‘Estimating unknown sparsity in compressed sensing’. Proc. of the 30th Int. Conf. on Machine Learning (ICML), 2013, pp. 217–225
- [13] Hurley, N., Rickard, S.: ‘Comparing measures of sparsity’, *IEEE Trans. Inf. Theory*, 2009, **55**, (10), pp. 4723–4741
- [14] Wang, Z., Bovik, A.C., Sheikh, H.R., et al.: ‘Image quality assessment: from error visibility to structural similarity’, *IEEE Trans. Image Process.*, 2004, **13**, (4), pp. 600–612